

# Nitrogenation of Silicon Carbide Layers Deposited on Silicon Single-Crystal Wafers via Pyrolysis of Poly(methylsilane)

Mihai Scarlete, Ian S. Butler,\* and John F. Harrod\*

Department of Chemistry, McGill University, 801 Sherbrooke Street West,  
Montreal, Quebec, Canada H3A 2K6

Received December 20, 1994. Revised Manuscript Received March 20, 1995<sup>®</sup>

Poly(methylsilane) (PMS), produced by the  $(\eta^5\text{-C}_5\text{H}_5)_2\text{Zr}(\text{CH}_3)_2$ -catalyzed dehydrocoupling of  $\text{CH}_3\text{SiHCl}_2$ , can be pyrolyzed into silicon carbide (SiC) and deposited as thin films on silicon single-crystal wafers to form SiC/Si heterojunctions. Two procedures have been developed for in situ doping the SiC layers in such heterojunctions with nitrogen. In the first, the Si-C bonds in a PMS sample containing 0.25 wt % of the organozirconium catalyst are partially converted into Si-N bonds by performing the pyrolysis in the presence of gaseous ammonia. The extent of nitrogenation of the polymer can be controlled by varying the  $\text{NH}_3$  partial pressure, and products with a wide range of resistivities are obtained. The second nitrogenation method involves amination of the residual Si-Cl bonds in a Wurtz-coupled prepolymer, prior to pyrolysis. Both nitrogen-doping methods afford thin layers of n-type materials. Films ranging in thickness from 100 nm to 2.5  $\mu\text{m}$  and resistivities ranging from 30 m $\Omega$  cm to 10  $\Omega$  cm have been obtained. FT-IR spectroscopy, SEM, and EDX, together with ellipsometry, have been used to monitor the progress of the pyrolyses and to characterize the new materials produced. Additional information on the composition of the new materials has been obtained from  $^{29}\text{Si}$  MAS-NMR spectroscopy and AFM measurements.

## Introduction

There are two intrinsic properties of silicon carbide (SiC) that make it a particularly promising semiconductor material for electronics applications. First, its bandgap, which lies between 2.2 and 3.0 eV depending on the SiC polytype, is much larger than is that for silicon (~1.1 eV). This means that electronic devices incorporating SiC technology can be operated at much higher temperatures than is possible with those based on silicon. For example, operating temperatures around 1000 °C are expected for SiC systems if only the thermal activation mechanism of the charge carriers is to be taken into consideration. The second important property of SiC is its good chemical stability, even under such harsh conditions as highly oxidizing atmospheres and high radiation fluxes. Moreover, SiC has excellent characteristics for high-frequency devices which can then compete favorably with GaAs-based products. The main driving force behind the research effort on SiC in recent years has been its potential in aerospace applications. Many SiC-based electronic devices have been developed, including smart sensors for hot engines, high-power and high-frequency systems,<sup>1</sup> MOSFET,<sup>2</sup> HBT,<sup>3</sup> photoreceptors and LEDs,<sup>4</sup> and p-i-n solar cells<sup>5</sup> (based on the transparency of polycrystalline  $\beta$ -SiC to

visible light above 0.5  $\mu\text{m}$ <sup>6</sup>). Economic interest in the production of SiC-based electronic devices is high because of the close similarity to semiconductor silicon processing (doping, lithography, ohmic contacts), allowing use of the infrastructure already in place for silicon technology which is currently underused.

Structured (single crystalline, polycrystalline, or microcrystalline) semiconductor-grade SiC layers are currently produced primarily by chemical vapor deposition (CVD),<sup>7</sup> vapor-phase epitaxy (VPE),<sup>8</sup> molecular beam epitaxy (MBE),<sup>9</sup> glow discharge,<sup>10</sup> or sputtering processes.<sup>11</sup> Still, there is considerable interest in the development of new synthetic routes to thin films of SiC. Routes that involve polymeric precursors are especially considered, because of their successful application in the formation of bulk amorphous SiC (a-SiC) and SiC fibers.

(4) Hamakawa, Y. Springer Processing in Physics 43; *Proceedings of the 2nd International Conference on Amorphous and Crystalline Silicon Carbide and Related Materials* (ICASC, 88); Rahman, M. M., Yang, C. Y.-W., Harris, G. L., Eds.; Springer-Verlag: Berlin, 1989; p 164.

(5) Solangi, A.; Chaudhry, M. *J Mater. Res.* **1992**, *7*, 247.

(6) Tawada, Y.; Kondo, M.; Okamoto, H.; Hamakawa, Y. *Solar Energy Mater.* **1982**, *6*, 299.

(7) Hattori, Y.; Kruangam, D.; Katoh, K.; Nitta, Y.; Okamoto, H.; Hamakawa, Y. *Proc. 19th IEEE Photovoltaic Specialists Conf.*; New Orleans, 1987; p 689.

(8) Kimoto, T.; Nishino, H.; Yamashita, A.; Woo, W. S.; Matsunami, H. Springer Proceedings in Physics 71; *Proc. Amorphous and Crystalline Silicon Carbide IV*; Yang, C. Y., Rahman, M. M., Harris, G. L., Eds.; Springer-Verlag: Berlin, 1989; p 31.

(9) Rowland, L. B.; Tanaka, S.; Kern, R. S.; Davis, R. F. Springer Proceedings in Physics 71; *Proc. Amorphous and Crystalline Silicon Carbide IV*; Santa Clara, CA, 1992; p 84.

(10) Tran, A. Springer Proceedings in Physics 34; *Proc. Amorphous and Crystalline Silicon Carbide I*; Harris, G. L., Yang, C. Y.-W., Eds.; Springer-Verlag: Berlin, 1989; p 167.

(11) Manning, B. M.; Hewitt, S. B.; Tarr, N. G.; MacElwee, T. W. Springer Proceedings in Physics 71; *Proc. Amorph. Cryst. Silicon Carbide IV*; Yang, C. Y., Rahman, M. M., Harris, G. L., Eds.; Springer-Verlag: Berlin, 1989; p 252.

<sup>®</sup> Abstract published in *Advance ACS Abstracts*, May 15, 1995.

(1) Palmour, J. W.; Edmond, J. A.; Kong, H. S.; Carter, C. H. Springer Proceedings in Physics 71; *Proc. Amorphous and Crystalline Silicon Carbide IV*; Yang, C. Y., Rahman, M. M., Harris, G. L., Eds.; Springer-Verlag: Berlin, 1992; p 289.

(2) Powell, J. A.; Matus, L. G. Springer Proceedings in Physics 34; *Proceedings of the 1st International Conference on Amorphous and Crystalline Silicon Carbide and Related Materials* (ICASC, 87); Harris, G. L., Yang, C. Y.-W., Eds.; Springer-Verlag: Berlin, 1989; p 2.

(3) Sasaki, K.; Fukazawa, T.; Furukawa, S. *Intl. Electron devices Meeting, Washington D.C.; Tech. Dig.* **1987**, 186.

Most of the current polymeric precursors do not have 1:1 silicon-to-carbon ratios, and consequently the resulting ceramic materials have an excess of one component over the other.<sup>12,13</sup> Among the known polymeric precursors, poly(methylsilane) ( $[\text{SiH}(\text{CH}_3)]_n$ , PMS) is a singularity, due to its initial Si-to-C ratio equal to the requisite 1:1 value. Pyrolysis of PMS under  $\text{N}_2$  containing a small amount of the organometallic catalyst used in its original synthesis was found to preserve this ratio and to yield a stoichiometric SiC product.<sup>14-17</sup> However, there are still two drawbacks to this process: (1) the technical difficulties related to the handling of highly air- and moisture-sensitive compounds; (2) removal of the residual organometallic species in the final product. Nevertheless, it is possible to synthesize electronic-grade SiC precursor (based on the criteria of oxygen content and concentration of electrically active impurities) by using the procedure outlined above and standard laboratory equipment. A direct consequence associated with the use of PMS, as opposed to any other precursor to date, is the possibility of monitoring incipient stages of oxidation by vibrational spectroscopy.<sup>18</sup>

Before the excellent semiconductor properties of SiC can be fully exploited in the production of electronic devices, a reliable doping procedure has to be developed. Nitrogen is electrically active in SiC and is a preferred donor because of its high solubility and relatively low ionization energy ( $\sim 70$  meV). In SiC/Si heterojunctions, the resistivity of the SiC layers is crucial and has to be strictly and reproducibly controlled. Resistivity control is usually achieved by diffusing the dopants into previously formed SiC layers by using spin-on-dopant (SOD) techniques. However, the SOD approach is not always applicable.<sup>5</sup> For example, when a SiC/Si heterojunction for solar cells is required, in situ doping is essential for reducing resistive losses and increasing the filling factor.<sup>5</sup> An alternative in situ route, which presumably could be applied to polymeric precursors, is the reaction of these precursors with boron or phosphorus compounds prior to pyrolysis.<sup>19</sup> Unfortunately, details of such doping procedures have not been fully described in the open literature. To our knowledge, there have been no procedures reported for the in situ doping of the growing SiC layers from polymeric precursors. We have developed such a doping procedure which can be performed at the same time as the pyrolysis. This one-step approach is based on earlier observations that annealing organosilanes, which initially contain no nitrogen, under  $\text{NH}_3$ , results in the elimination of the organic groups attached to the silicon precursor.<sup>20-23</sup> This process,

which takes place at 400–600 °C, has already been successfully employed in the production of pure silicon nitride ( $\text{Si}_3\text{N}_4$ ).<sup>24-26</sup>

The presence of functional groups on the precursor material is vital for the cross-linking and doping steps, as well as for promoting adhesion to substrates. Poly(methylsilane) is also an outstanding candidate from these points of view. The initial presence of Si–H bonds, besides being beneficial for the adhesion properties to the Si substrate, leads to specific features in the thermally induced cross-linking process occurring during the pyrolysis of PMS, compared, for example, to the pyrolysis of poly(carbosilane) (PCS). The bifunctionality of Si in terms of its cross-linking properties has already been noted.<sup>27,28</sup> Other studies have shown that SiC formation is controlled by the formation of HSi–SiH bonds leading to the cross-linking of polymer chains.<sup>29</sup> The presence of catalytic amounts of  $(\eta^5\text{-C}_5\text{H}_5)_2\text{Zr}(\text{CH}_3)_2$  in PMS is particularly effective in favoring formation of Si–C rather than Si–Si bonds during pyrolysis, thus reducing the Si excess to give stoichiometrically pure SiC.

In the present work, we have utilized the intrinsic functional groups on PMS (Si–H and Si– $\text{CH}_3$ ) in the presence of the organozirconium catalyst, or additional built-in functionalities such as chlorine end-capping of a Wurtz prepolymer in a one-step process (in contrast to the two-step process reported earlier<sup>30</sup> which involves doping prior to pyrolysis) to produce SiC layers and in situ nitrogen-doped SiC layers coated on Si single-crystal wafers.

## Experimental Section

Poly(methylsilane) was prepared according to the literature procedure,<sup>15</sup> i.e., sodium coupling of  $\text{CH}_3\text{SiHCl}_2$  followed by  $\text{LiAlH}_4$  reduction of the residual chlorine. Cross-linked samples (obtained by anionic cross-linking of the Wurtz coupled prepolymer, promoted by  $\text{LiAlH}_4$ ) and soluble polymers prepared by further polymerization of the Wurtz prepolymer with  $(\eta^5\text{-C}_5\text{H}_5)_2\text{Zr}(\text{CH}_3)_2$  were subjected to pyrolysis. A typical pyrolysis cycle consisted of two stages: (1) the heating rate was set at 2–5 °C/min up to 450 °C, followed by maintaining the sample at 450 °C for 1 h in order to produce poly(carbosilane); (2) the heating rate was increased to 8 °C/min until 1100 °C was reached, and then the sample was maintained at this temperature for a further 90 min. The pyrolyses were performed under different atmospheres, e.g., UHP Ar,  $\text{NH}_3$ , 7%  $\text{H}_2/\text{Ar}$ , and varying mixtures of  $\text{N}_2/\text{NH}_3$  and  $\text{Ar}/\text{NH}_3$ . Prepurified  $\text{NH}_3$  (Matheson) was passed immediately prior to use through a column (1.5 m long, 7.6 mm diameter) of KOH pellets and 4 Å molecular sieves at rates of 10–200 mL/min.

The polished side of silicon single crystal wafers—10 cm diameter, 1–3° off-oriented [100], 20 Ω cm P(B), polished on

(12) Thorne, K. J.; Johnson, S. E.; Zheng, H.; Mackenzie, J. D.; Hawthorne, M. F. *Chem. Mater.* **1994**, *6*, 110.

(13) Laine, R. M.; Babonneau, F. *Chem. Mater.* **1993**, *5*, 260.

(14) Zhang, Z.-F.; Babonneau, F.; Laine, R. M.; Mu, Y.; Harrod, J. F.; Rahn, J. A. *J. Am. Ceram. Soc.* **1991**, *74*(3), 31, 670.

(15) Mu, Y.; Laine, R. M.; Harrod, J. F. *Appl. Organomet. Chem.* **1994**, *8*, 95.

(16) Seyferth, D.; Wood, T. G.; Tracy, H. J.; Robinson, J. J. *J. Am. Ceram. Soc.* **1992**, *75*, 1300.

(17) Hengge, E.; Wienberger, M. *J. Organomet. Chem.* **1992**, *433*, 21.

(18) Scarlete, M.; Brienne, H. R.; Harrod, J. F.; Butler, I. S. *Chem. Mater.* **1994**, *6*, 977.

(19) Chu, C. J.; Ting, S. J.; Mackenzie, J. D.; Springer Proceedings in Physics 71; *Proc. Amorph. and Cryst. Silicon Carbide IV*; Yang, C. Y., Rahman, M. M., Harris, G. L., Eds.; Springer-Verlag: Berlin, 1989; p 93.

(20) Brown-Wensley, K. A.; Sinclair, R. A. US Patent No. 4537942, 1985.

(21) Bujalski, R. J. D. European Patent Application 200326, 1986.

(22) Burns, G. T.; Chandra, G. *J. Am. Ceram. Soc.* **1989**, *72*(2), 333.

(23) Varshney, S. K.; Beatty, C. L. *Proc. 6th Annual Conference on Composites and Advanced Ceramic Materials*; Cocoa Beach, FL, 1989; p 555.

(24) Okamura, K.; Sato, M.; Hasegawa, Y. *Ceram. Int.* **1987**, *13*, 55.

(25) Han, H. N.; Lindquist, D. A.; Haggerty, J. S.; Seyferth, D. *Chem. Mater.* **1992**, *4*, 705.

(26) Schmidt, W. R.; Marchetti, P. S.; Interrante, L. V.; Hurley, W. J., Jr.; Lewis, R. H.; Doremus, R. H.; Maciel, G. E. *Chem. Mater.* **1992**, *4*, 937.

(27) Boury, B.; Carpenter, L.; Corriu, R. *Angew. Chem., Int. Ed. Eng.* **1990**, *29*(7), 785.

(28) Boury, B. R.; Leclercq, D.; Mutin, P. H.; Planeix, J. M.; Vioux, A. *Organometallics* **1991**, *10*, 1457.

(29) Corriu, R.; Leclercq, D.; Mutin, P. H.; Planeix, J. M.; Vioux, A. *Organometallics* **1993**, *12*, 45.

(30) Chu, C. J.; Ting, S. J.; Mackenzie, J. D. *Springer Proc. Phys.* **1992**, *56. Amorphous and Crystalline Silicon Carbide III*; Harris, G. L., Spencer, M. G., Young, C. Y., Eds.: 87.

one side and etched on the other—was used as the coating surface. Special precautions were taken with respect to the creation of a hydrophobic surface adapted for promoting the initial adhesion to the Si-H functions in the precursor. The substrates were cleaned initially with a  $\text{H}_2\text{SO}_4/\text{H}_2\text{O}_2$  (5:1) solution at 95 °C for 5 min to remove adsorbed residual organic materials, cascade rinsed in deionized water, etched in a solution of  $\text{H}_2\text{O}/\text{HF}$  48% (5:1) for 4 min, and finally rinsed with acetone. EDX measurements showed a negligible amount of oxygen present after 1 min, but verification of fine oxide removal was established from the wetting properties of a dodecane/Si interface by contact angle goniometry. Before coating, the wafers were dried and temperature stabilized in ultrahigh-purity Ar at 850 °C for 30 min to create a less hydrophilic (i.e., inert to hydroxyl group adsorption) surface.<sup>31</sup>

Two coating procedures were used: (1) a deposition technique involving the transport of the volatile species formed by thermal cracking of PMS during the pyrolysis under  $\text{NH}_3$  to the substrate located at the cold end of the horizontal furnace; (2) spin coating with mixtures of the aminated Wurtz prepolymer and the PMS. The purity of the starting polymers was established by comparison of their IR spectra with those previously reported,<sup>15,18,32</sup> while the degree of initial cross-linking was determined by  $^1\text{H}$  NMR spectroscopy. The pyrolyses were performed in a Lindberg single-zone programmable furnace equipped with a Eurotherm PID temperature controlled which could be operated up to 1100 °C with an accuracy of  $\pm 1$  °C at 1100 °C. EDX measurements were used to determine the elemental composition of the layers obtained. Identical samples of bulk material were pyrolyzed at the same time as the coated wafers, and  $^{29}\text{Si}$  MAS NMR spectroscopy was used to detect the presence of SiC,  $\text{Si}_3\text{N}_4$ ,  $\text{SiO}_2$ , and elemental Si in the resulting powders. The texture of the SiC was examined by scanning electron microscopy (SEM), while atomic force microscopy (AFM) was used to obtain a statistical characterization of the topology of the surface. The thicknesses (less than 500 nm) of the mirrorlike layers obtained via vapor deposition were determined by ellipsometry, and a Sloan-Dektak profilometer was used for evaluating the thickness of the spin coated layers (in the micrometer range). The resistivities of the coatings were measured with a four-point probe, and the conductivity type was determined by EFM (hot probe) measurements. FT-IR spectra ( $4\text{ cm}^{-1}$  resolution) were recorded on a Bruker IFS-48 spectrometer equipped with a microscope, DTGS detector, and a SONY-Trinitron PVM 1340 color monitor for spectral display.

## Results and Discussion

**Deposition of a-SiC Layers on Silicon Single-Crystal Wafers.** Typical EDX spectra of the polished sides of the as received Si single-crystal wafers, and the surfaces of the substrates after 1 min etch in HF are shown in Figure 1. There was no evidence of oxide for the penetration depth of the EDX experiments. However, the etched surface exhibited a variable contact angle ( $84\text{--}74^\circ$ ) with dodecane when subjected to a further etch in HF for times ranging from 1 to 4 min. Longer etching times did not lead to any further changes in contact angle. The greater sensitivity of the contact angle method compared to EDX for detecting residual oxide on silicon surfaces was used in deciding on the etching time in HF of 4 min rather than 1 min, as was used previously.<sup>18</sup>

Thin SiC films were obtained via pyrolysis of PMS under Ar or  $\text{N}_2$ , both by vapor deposition of the volatile species generated during thermal cracking of the polymer and by spin coating. The SiC layers deposited by vapor deposition (thicknesses of a few hundred nanometers) exhibited a mirrorlike appearance. Statistical

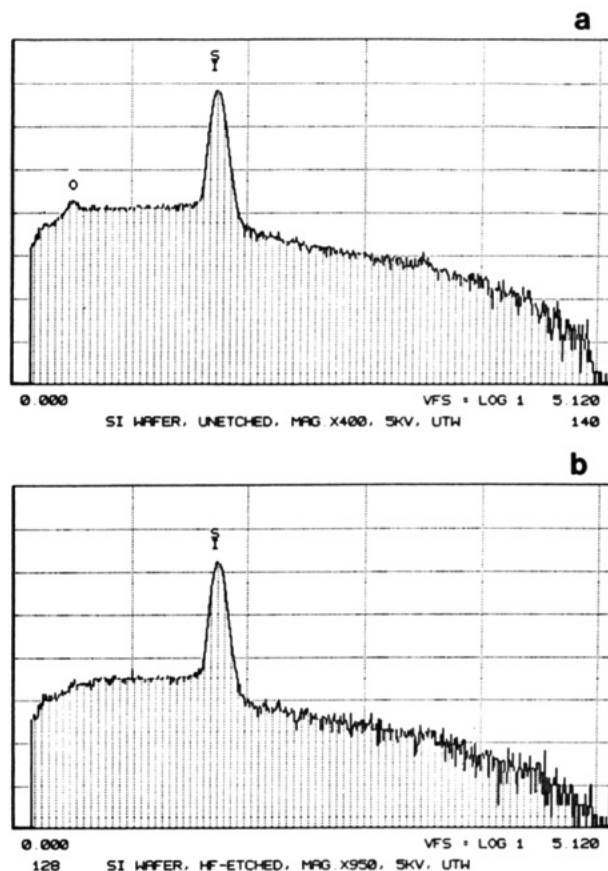


**Figure 1.** EDX spectra of a Si single-crystal wafer: (a) as received (magnification  $\times 400$ , 5 kV, UTW); (b) after HF etching (magnification  $\times 950$ ; 5 kV, UTW).

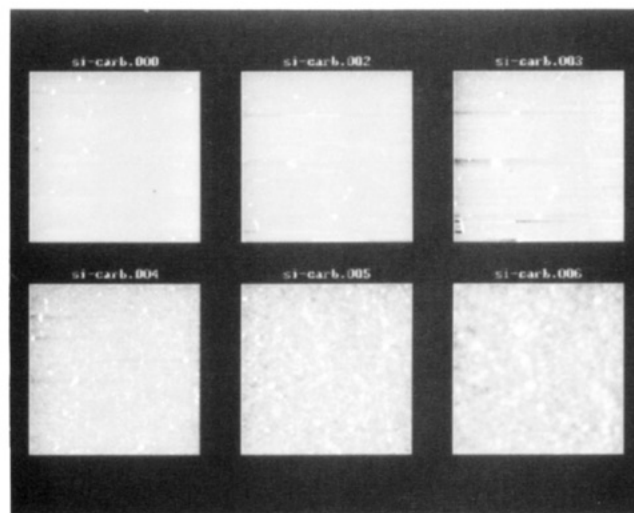


**Figure 2.** AFM images of a SiC layer prepared by pyrolysis of a spin-coated film of PMS on a Si substrate at different resolutions (nm): (1) 10, (2) 5, (3) 3, (4) 2, (5) 1, (6) 0.8.

analysis using atomic force microscopy (AFM) indicated a flat surface to within  $\pm 2.5\%$  (Figure 2, images 1–6) for the films formed by vapor deposition. The roughness of the spin-coated layers was  $\pm 10\%$  (profilometer data) for films of about  $1\ \mu\text{m}$  thick. The EDX spectrum of a coated silicon single crystal wafer is shown in Figure 3, while its FT-IR spectrum is illustrated in Figure 4. The appearance of a broad IR band at  $\sim 800\text{ cm}^{-1}$  is indicative of SiC formation.<sup>14,33–36</sup> The resistivities of the

(31) Hair, M. L. *Silanes Surfaces and Interfaces*; Leyden, D. E., Eds.; Gordon and Breach Science Publishers: New York, 1986; p 29.

(32) Mu, Y. Ph.D. Thesis; McGill University, 1991.

(33) Hasegawa, Y.; Yimura, M.; Yajima, S. *J. Mater. Sci.* **1980**, *15*, 720.

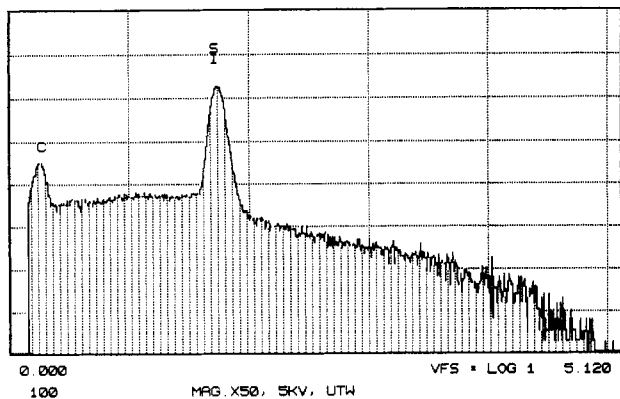


Figure 3. EDX spectrum of a vapor deposited SiC layer (thickness  $\sim 450$  nm; magnification  $\times 50$ ; 5 kV, UTW).

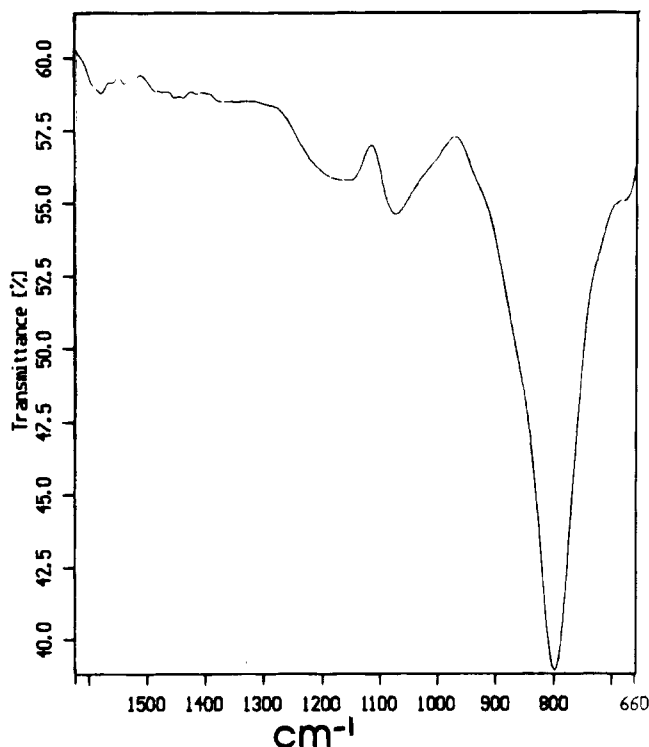


Figure 4. FT-IR spectrum of a vapor deposited SiC layer coated on a Si single-crystal wafer. The band at  $800\text{ cm}^{-1}$  is characteristic for SiC. The two bands at  $1100$  and  $1200\text{ cm}^{-1}$  are indicative of adventitious oxidic and graphite phases, respectively.

vapor deposited layers were in the range of  $10^6\ \Omega\text{ cm}$ , and no correlation with the thickness was observed. The slightly smaller and variable resistivities ( $10^4$ – $10^5\ \Omega\text{ cm}$ ) measured for the films produced in a  $\text{N}_2$  atmosphere suggests parasitic nitrogen incorporation from  $\text{N}_2$ , or adventitious out-diffusion of the dopant from the substrate. The additional IR band located at  $1100$ – $1000\text{ cm}^{-1}$  is attributed to the presence of adventitious oxygen in the SiC layer, since oxidation of the Si substrate leads to a sharp absorption at  $1107\text{ cm}^{-1}$  and, from our previous work on the PMS precursor, oxidation of the polymer prior to pyrolysis also results in a product with a sharp IR band at  $1107\text{ cm}^{-1}$  (the sharpness is believed to be associated with the high mobility of the precursor

on the Si surface<sup>18</sup>). The assignment was suggested by previous observations of a similar absorption band at  $\sim 1000\text{ cm}^{-1}$  during the oxidation of SiC crystals.<sup>37</sup> The broad weak band in the  $1200$ – $1100\text{ cm}^{-1}$  region is attributed to graphite formation resulting from a small amount of carbon excess. The relative sharpness of the SiC band should be emphasized at this point; for example, polycrystalline SiC films obtained by laser ablation deposition (LAD), even after annealing, exhibit an IR band roughly 3 times wider than that observed in this case.<sup>38</sup>

A bulk sample of the PMS precursor, pyrolyzed simultaneously with the coated wafer was examined by  $^{29}\text{Si}$  MAS NMR spectroscopy to determine if there was excess Si (PMS pyrolyses do not result in carbon excess in the residual material) or  $\text{SiO}_2$  present after pyrolysis. In agreement with earlier work,<sup>14</sup> no signals due to elemental Si ( $-80$  ppm) or  $\text{SiO}_2$  ( $-100$  ppm) were detected for this material. The resonances appearing at about  $-20$  ppm indicated quantitative SiC formation. The preservation of Si–C bonds in the residue (due to the presence of the catalyst) is valid also for the volatile species leading to the coated layers, despite the unlikelihood of some of the organozirconium catalyst being present in the volatile species. The resistivities of the “undoped” spin-coated layers were in the  $10^2$ – $10^3\ \Omega\text{ cm}$  range, and this drop can be associated with charge carriers related to carbon, catalyst, or oxygen. The detection of oxygen in the IR measurements but not in the NMR experiments is not surprising since very low concentrations of interstitial oxygen ( $5 \times 10^{17}$  – to  $1 \times 10^{18}$  atoms/ $\text{cm}^3$ ) can be detected by FT-IR spectroscopy,<sup>39</sup> due to the high extinction coefficient of  $\nu_{\text{as}}(\text{Si}-\text{O}-\text{Si})$  and the unavoidable formation of Si–O–Si units during the oxidation of SiC. The crystallinity of the SiC layers was not of particular concern in this work, even though the above-mentioned unusual mobility of the precursor on the silicon surface might be exploited to give a higher degree of crystallinity. AFM measurements at higher magnification revealed that the material was amorphous (Figure 2, images 4–6). Since it is already known that crystalline SiC films can be grown below  $1000\text{ }^\circ\text{C}$  from single-source CVD precursors,<sup>40</sup> we would also expect that crystallinity could be achieved with the present system.

**Nitrogenation of Silicon Carbide Layers Deposited on Silicon Single-Crystal Wafers. *In Situ, Gas-Phase Nitrogenation during Pyrolysis.*** Partial conversion of the Si–C bonds into Si–N bonds under a carefully controlled partial pressure of  $\text{NH}_3$  in the gas phase was used to control the amount of nitrogen being admitted into the growing SiC layer. By using partial pressures of  $\text{NH}_3$  in a carrying Ar stream, silicon single-crystal wafers coated with heavily nitrogenated SiC layers could be produced. When the mole fraction of  $\text{NH}_3$  was in the  $0.1$ – $0.01$  range, the resistivities dropped dramatically from those obtained in an Ar atmosphere, from  $10\ \Omega\text{ cm}$  to  $30\ \text{m}\Omega\text{ cm}$ , corresponding to concentra-

(34) Lipowitz, J. *Proceedings of the XXVII Organosilicon Symposium*; March 18–19, 1994, Rensselaer Polytechnic Institute: Troy, NY, p B-23.

(35) Schmidt, W. R.; Interrante, L. V.; Doremus, R. H.; Trout, T. K.; Marchetti, P. S.; Maciel, G. E. *Chem. Mater.* **1991**, *3*, 257.

(36) Narsavage, D. M.; Interrante, L. V. *Chem. Mater.* **1991**, *4*, 721.

(37) Lee, S.; Hench, L. L. In *Ultrastructure and Processing of Advanced Structural and Electronic Materials*; Noyes: Park Ridge, NJ, 1983; p 171.

(38) El Kakani, M. A.; Chaker, M.; Boily, S.; Papadopoulos, A.; Huai, Y.; Jean, A. *Mater. Res. Soc. Symp. Proc.*; Materials Research Society: Pittsburgh, 1993; Vol. 306, p 211.

(39) Annual Book of ASTM Standards, 1990, 10.05, F1188-88.

(40) Larkin, D. J.; Interrante, L. V. *Springer Proceedings in Physics; Amorphous and Crystalline Silicon Carbide*; Yang, C. Y., Rahaman, M. M. Harris, G. L., Eds.; Springer-Verlag: Berlin, 1989; p 239.

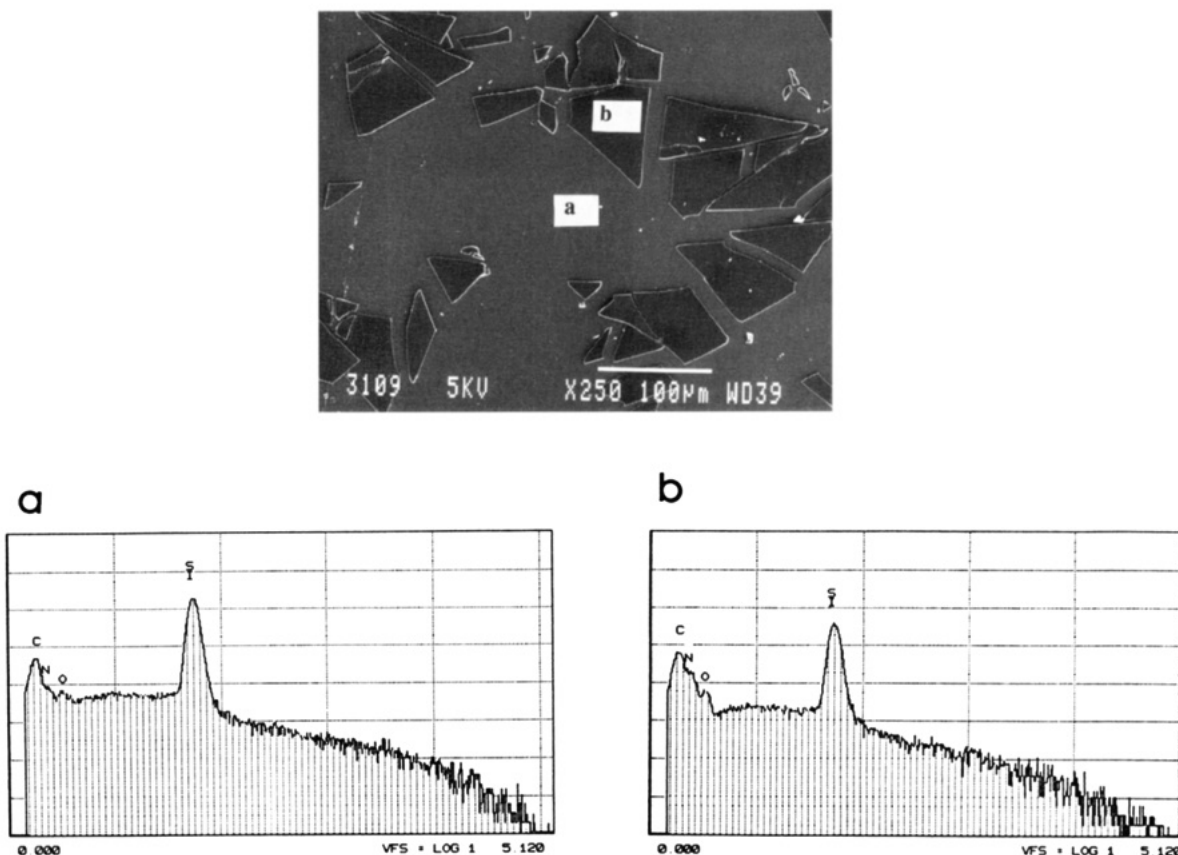


**Figure 5.** SEM micrograph of a nitrogenated, vapor deposited SiC film deposited in an  $\text{NH}_3/\text{Ar}$  atmosphere. Spot EDX analyses of (a) the continuous film on the Si substrate and (b) the upper shattered film are indicative of an unidirectional growth from the substrate with effective segregation coefficients lower than 1 for both oxygen and nitrogen.

tions of  $10^{18}$ – $10^{16}$  donors/cm<sup>3</sup>, respectively.<sup>41</sup> A 100% dispersion in the resistivity was achieved for substrates with areas of 2 cm<sup>2</sup>. The effect is probably due to a variable gas-flow regime. This assumption is based on close similarities with the variations in the dopant profiles obtained in the silicon crystals due to unstable melt-flow patterns of the molten silicon during the growth process. Since standard flow meters were used to control the pressure and flow rates and no special precautions were taken to ensure the mixing of components in the gas phase, improved results could be expected if mass flow controllers (MFC) are used and the design for the geometry of the furnace is adapted to the restrictions of the flow. When the mole fraction of  $\text{NH}_3$  of  $\sim 0.15$  was employed during pyrolysis, a more complicated situation arose as indicated by the SEM image and EDX spectra of a typical coating for these conditions (Figure 5). Two separate layers were formed on the substrate which were targeted in the EDX experiments. The two spotted areas highlighted in the SEM micrograph gave the spot-EDX spectra for (a) the continuous layer and (b) the shattered film. The relative concentrations of both nitrogen and oxygen were clearly greater in the top layer, eliminating the possibility of surface contamination during manipulation and/or analysis (in this case, only oxygen contamination should be observed). Moreover, since the thermal decomposition of  $\text{NH}_3$  at a higher temperature should lead to a decreased amount of nitrogen in the upper

layers in the growing SiC film, a reasonable explanation would be that both the excess nitrogen (i.e., that beyond the solubility limit in SiC) and adventitious oxygen present during the experiment were segregated into the emerging phase upon cooling. The pronounced segregation of the major impurities (nitrogen and oxygen) in the top layer suggests a unidirectional crystallization process which starts from the substrate and involves distribution coefficients lower than 1. The clear delimitation of the two layers can be attributed to two immiscible “carbide-like” and “nitride-like” phases (denomination based on the known fact that the two limiting compositions,  $\text{Si}_3\text{N}_4$  and SiC exclude each other). The homogeneous texture of the underneath phases indicates that a significant amount of nitrogen can be homogeneously incorporated (on the SEM scale) into the SiC lattice, in accordance with the high levels of doping observed during the above experiments. Infrared spectroscopy did not provide any additional information on the presence and type of bonding of nitrogen, because the characteristic vibrational modes of Si–N expected<sup>42–44</sup> at  $\sim 950$ , 835, and 800  $\text{cm}^{-1}$  were buried under the much more intense, broad absorption at 800  $\text{cm}^{-1}$  due to the amorphous SiC layer. Several bulk precursor samples, which were pyrolyzed simultaneously with the layers, were examined by <sup>29</sup>Si MAS NMR spectroscopy. A variety of  $\text{SiC}_x\text{N}_y$  materials, ranging from pure SiC to pure  $\text{Si}_3\text{N}_4$ , were produced

(42) Naiman, M. L.; Kirk, C. T.; Aucoin, R. J.; Terry, F. L.; Senturia, S. D. *J. Electrochem. Soc.* **1984**, *131*, 637.

(43) Rocheleau, R. E.; Zhang, Z. *J. Appl. Phys.* **1992**, *72*(1), 282.

(44) Marchand, A.; Forel, M. T.; Metras, F.; Valade, J. *J. Chim. Phys.* **1964**, *61*(3), 343.

(41) Compensation and grain-boundary effects were not determined; their contributions can be considered not to affect significantly the concentration of charge carriers at resistivities in the order of m $\Omega$  cm.



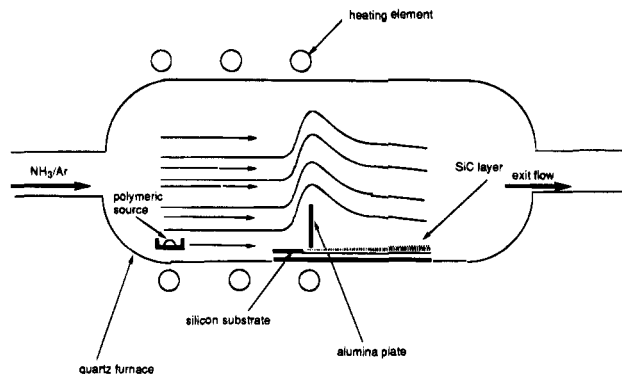


**Figure 6.** Procedure used to form a pronounced thickness gradient in the SiC layer. The imposed pattern for the gas flow renders the deposition rate a function of the location of the deposition area with respect to the alumina plate.

depending on not only the  $\text{NH}_3$ /carrier gas molar ratio but also on other conditions such as the flow rate, the annealing program or the size of the samples. These dependences will form the subject of a future publication. Characteristic  $^{29}\text{Si}$  NMR signals for  $\text{SiC}^{45-48}$  (a structured band at  $-20$  ppm) and  $\text{Si}_3\text{N}_4^{49}$  (a featureless, broad band at  $-50$  ppm) or a band envelope with substructures at  $-47$  and  $-49$  ppm) were observed for the limiting cases. There was no NMR evidence for the presence of any elemental silicon ( $-80$  ppm) or  $\text{SiO}_2$  ( $-100$  ppm) in all the pyrolysis products.

The detection of nitrogen in a SiC lattice (e.g., shallow donors in SiC-based semiconductor devices) is usually quite a difficult task. Although  $^{13}\text{C}$  and  $^{29}\text{Si}$  NMR spin-lattice relaxation measurements have been used to detect the location of nitrogen in 6H-polytype SiC,<sup>50</sup> indirect methods such as the Hall effect,<sup>51,52</sup> photoluminescence,<sup>53</sup> or EPR measurements<sup>54</sup> normally have to be used. Attempts have been made to relate the IR bands appearing at very low temperatures (7–80 K) to different nitrogen locations in the SiC lattice.<sup>55</sup> A special deposition procedure was developed in this work, based on the observed sharpness of the SiC band for very thin films. In this procedure, an atmosphere of Ar and  $\text{NH}_3$  (10:1) was used, and gas flow over the substrate was baffled by a small alumina plate, placed perpendicular to the substrate surface as shown in Figure 6. In this way, different areas were rendered inaccessible for the gas flow, leading to very slow deposition rates. This experiment led to a pronounced gradient in the thickness of the deposited SiC layer with some areas being coated to a thickness of only  $\sim 20$  nm.

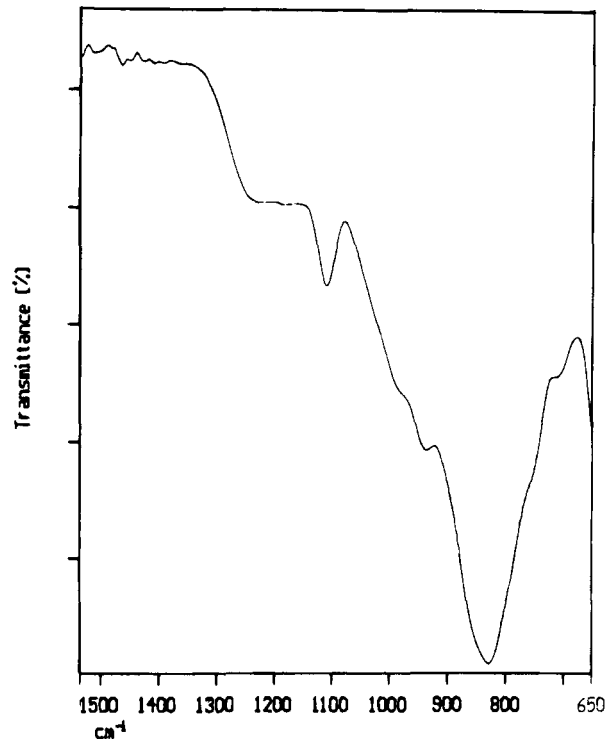


**Figure 7.** FT-IR spectrum of a nitrogenated, vapor deposited SiC layer on Si single-crystal wafer; the absorption at  $939\text{ cm}^{-1}$  is characteristic for  $\nu(\text{Si-N})$ .

The combined effect of considerable nitrogen insertion due to the high molar fraction of  $\text{NH}_3$  (0.10) present in the gas phase during the pyrolysis and the resulting ultrathin SiC layers led to the structured IR-absorption band shown in Figure 7. The shift in the  $\nu(\text{SiC})$  band to  $822\text{ cm}^{-1}$  suggests the formation of a silicon carbonitride species. The shift of the antisymmetric SiC mode toward higher wavenumbers is consistent with the expected increase in the force constant of the Si–C bond in the series Si–C–Si, C–Si–N and provides additional support for the limited solubility of nitrogen in SiC, as suggested by the SEM micrograph. In addition, a new band was detected at  $939\text{ cm}^{-1}$  (Figure 7). This additional band is characteristic for the Si–N stretch and, to our knowledge, is the first direct time that nitrogen in SiC layers has been detected by IR spectroscopy at room temperature.

**Ammination of the Wurtz Prepolymer.** A second route for the in situ introduction of nitrogen into SiC layers involves ammination of a prepolymer produced by Wurtz dehalocoupling of  $\text{CH}_3\text{SiHCl}_2$ . If stoichiometric amounts of sodium metal and monomer are used, the resulting polymer is chlorine end-capped.<sup>15,56</sup> The residual Si–Cl bonds are suitable sites for ammination by  $\text{NH}_3$ . Figure 8 illustrates the IR spectra of (a) the initial PMS, (b) the nitrogenation product,<sup>57</sup> and (c) a partially pyrolyzed sample. The presence of N–H groups in the amminated polymer is evident from the  $\nu(\text{N-H})$  stretch in spectrum (b) at  $3380\text{ cm}^{-1}$ . A shift of the Si– $\text{CH}_3$  symmetric deformation from  $1247$  to  $1270\text{ cm}^{-1}$  accompanies the nitrogenation reaction (a similar shift to  $1260\text{ cm}^{-1}$  was observed during oxidation of PMS<sup>18</sup>). A mixture of this amminated polymer and the

(45) Richardson, M. F.; Hartman, J. S.; Guo, D. *Can. J. Chem.* **1992**, *70*, 700.

(46) Zhang, H.; Pensl, G.; Glasow, P.; Leibenzeder, S. *Electrochem. Soc. Extended Abstr.* **1989**, 89–2, 714.

(47) Thompson, D. P. *J. Am. Ceram. Soc.* **1991**, *74*, 777.

(48) Wagner, G. W.; Na, B. K.; Vannice, M. A. *J. Phys. Chem.* **1989**, *93*, 5061.

(49) Olivieri, A. C.; Hatfield, G. F. *J. Magn. Reson.* **1991**, *94*, 535.

(50) Hartman, J. S.; Narayanan, A.; Wang, Y. X. *J. Am. Chem. Soc.* **1994**, *116*, 4019.

(51) Tachibana, T.; Kong, H. S.; Wang, Y. C.; Davis, R. F. *J. Appl. Phys.* **1990**, *67*, 6375.

(52) Alekseenko, M. V.; Zabrodskii, A. G.; Timofeev, M. P. *Sov. Phys. Semicond.* **1987**, *21*, 494.

(53) Choyke, W. J.; Patrick, L. *Phys. Rev.* **1962**, *127*, 1868.

(54) Carlos, W. E.; Moore, W. J.; Siebenmann, P. G.; Freitas, J. A., Jr.; Kaplan, R.; Bishop, S. G.; Nordquist, Jr. P. E. R.; Kong, M.; Davis, R. F. *Proc. Mater. Res. Soc. Symp.* **1987**, Anaheim, CA, 276.

(55) Suttrop, W.; Zhang, H.; Schadt, M.; Pensl, G.; Dohnke, K.; Leibenzeder, S. *Springer Proceedings in Physics 71; Proc. Amorphous and Crystalline Silicon Carbide IV*; Santa Clara, CA, 1992; p 143.

(56) Wood, T. G. Ph.D. Thesis, MIT, 1984.

(57)  $[\text{R}_3\text{Si-NH}_3]^+\text{Cl}^-$  groups in the sample and residual toluene are responsible for the additional bands at  $2400\text{ cm}^{-1}$  and, respectively,  $1900$  and  $3100\text{ cm}^{-1}$  in spectrum 8b, both removed during pyrolysis.

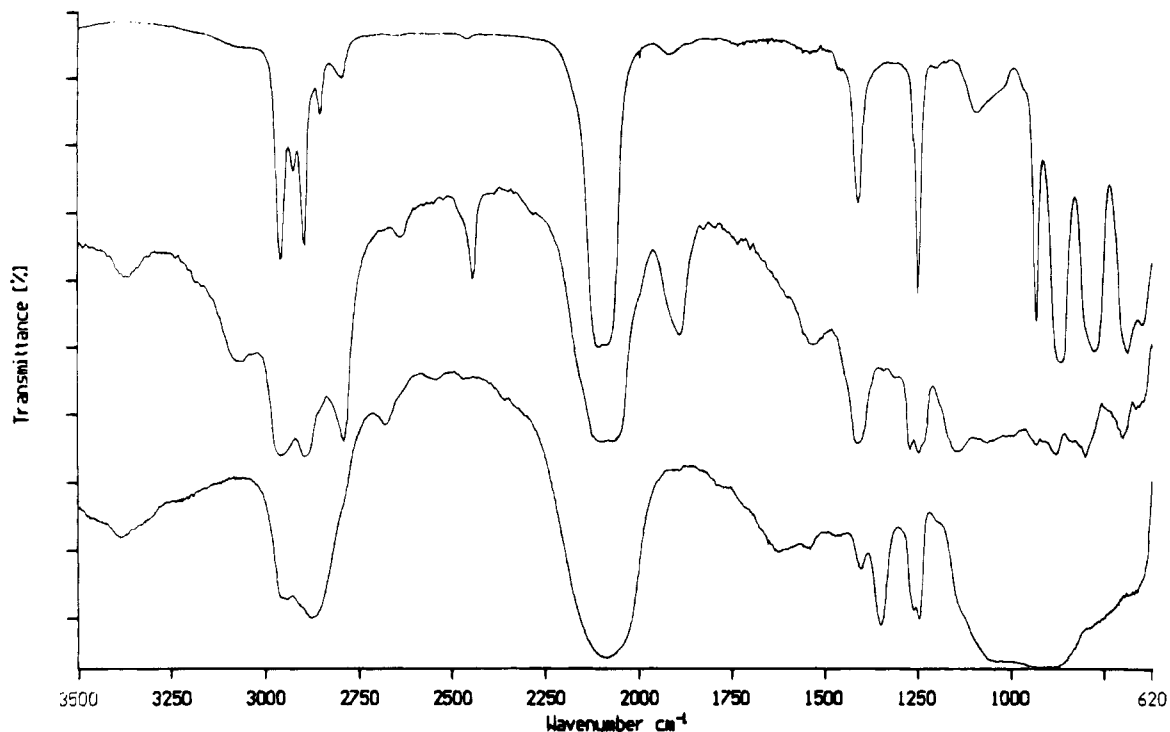


**Figure 8.** FT-IR spectra of (a) the starting polymer, (b) the aminated polymer, and (c) the polymer after partial pyrolysis of a spin coated at 300 °C. Evidence for the Kumada rearrangement is provided by the band at 1352  $\text{cm}^{-1}$ .

polymer produced by the  $(\eta^5\text{-C}_5\text{H}_5)_2\text{Zr}(\text{CH}_3)_2$ -catalyzed polymerization of the hydrogenated Wurtz prepolymer, was used in a spin-coating process. The pyrolysis was performed under inert atmosphere (UHP Ar) and the IR spectrum of a typical sample heated up to at 300 °C is shown in Figure 8c. The N–H stretching band remained detectable by IR up to 450 °C. The Kumada rearrangement,<sup>58</sup> which takes place below 400 °C during the pyrolysis of PMS, involves mainly transformations in the chain, and so the possible loss of the amino groups during the rearrangement has to be taken into account. The final stages of the Kumada formation of poly(carbosilane) are readily detected by the appearance of the  $\text{CH}_2$  scissoring mode in the IR spectrum at 1352  $\text{cm}^{-1}$ . Figure 8c reveals that the rearrangement has indeed taken place, and moreover the persistence of the  $\nu(\text{N-H})$  band at 3400  $\text{cm}^{-1}$  indicates that the nitrogen in the precursor has survived the rearrangement. The eventual disappearance of the  $\nu(\text{N-H})$  band at higher temperatures is most probably the result of dehydrocoupling between Si–H and N–H bonds. This supposition is supported by IR analyses of the simultaneous disappearance of the  $\nu(\text{N-H})$  and  $\nu(\text{Si-H})$  bands for  $\text{Si}_3\text{N}_4$  thin films formed by PECVD from  $\text{SiH}_4$  and  $\text{NH}_3$ ,<sup>45</sup> as well as its detection at higher temperatures in similar environments if more concentrated samples are used.<sup>25</sup> A large excess of Si–H bonds will lead to complete reaction of the N–H bonds, as has been observed for poly(carbosilazanes), where three-dimensional backbones are known to be formed by facile coupling of Si–H and N–H bonds, with the subsequent formation of  $\text{H}_2$  and the creation of  $\text{Si}_3\text{N}$  knots.<sup>59</sup> From the IR spectra, there was no evidence for such a process taking place because the  $\nu(\text{SiC})$  band could not be resolved sufficiently to detect the presence of nitrogen

after the pyrolysis. However, resistivities in the range 50  $\text{m}\Omega\text{ cm}$  to 5000  $\Omega\text{ cm}$  were obtained by varying the amounts (1–10%) of the Wurtz prepolymer dopant. These resistivities imply donor concentrations greater than  $10^{16}$  donors/ $\text{cm}^3$ , making this process of potential interest for doping SiC for use in solar cells, where the requirements related to the dispersion of the resistivity are more relaxed. However, the results were less reproducible than the gas-phase procedure because of inaccuracies in weighing the dopant and the presence of the impurities derived from residual catalyst and/or adventitious oxygen.

### Conclusions

Nitrogen concentrations in the range of interest for the production of SiC/Si heterojunctions have been obtained in a one-step process which involves the direct pyrolysis of PMS into n-type SiC layers deposited on silicon single-crystal wafers. Two procedures have been developed in situ doping of a-SiC layers for solar cells. Reproducible results have been obtained by controlling the  $\text{NH}_3$  partial pressure in the gas phase during the pyrolyses. Ammination of a prepolymer, prepared by Wurtz-type coupling of dimethyldichlorosilane, can also be used to synthesize dopant polymers. Pyrolysis under Ar of mixtures of these polymers with PMS produces nitrogen-doped SiC layers. Such layers exhibited resistivities typically in the range of 30  $\text{m}\Omega\text{ cm}$  to 10  $\Omega\text{ cm}$  for sample thicknesses varying from 100 nm to 2.5  $\mu\text{m}$ .

**Acknowledgment.** Dr. Graham McKinnon of Alberta Microelectronic Center is thanked for providing the Si single-crystal wafers used in this study. This research was supported by the Fonds FCAR du Québec, the Natural Sciences and Engineering Research Council of Canada, and Department of Energy, Mines and Resources (Canada).

CM940560V

(58) Shinu, K.; Kumada, M. *J. Org. Chem.* **1958**, *23*, 139.

(59) Pilot, J. P. *Proceedings of the International Symposium on Organosilicon Chemistry*; 1993; Poznan, 16.